Dalton Transactions

ROYAL SOCIETY OF CHEMISTRY

PAPER

View Article Online
View Journal | View Issue

Cite this: *Dalton Trans.*, 2021, **50**, 17625

Amino acid-derived bisphenolate palladium complexes as C–C coupling catalysts†

Eszter Fazekas, David T. Jenkins, Andrew A. Forbes, Brendan Gallagher, Georgina M. Rosair and Ruaraidh D. McIntosh *

A series of amine bisphenol (ABP) pro-ligands featuring amino acid ester pendant arms were prepared. Optimisation of the synthetic method allowed the facile incorporation of naturally occurring, chiral amino acids into the ABP scaffold with minimal racemisation. Reaction of the pro-ligands (LH_2) with $Pd(OAc)_2$, in the presence of amines, led to the formation of complexes with an unprecedented pincer-like O,N,O coordination mode around the Pd^{II} centre. The complexations in the presence of trialkylamines (NR_3) afforded a mixture of $LPdNR_3$ and $LPdNHR_2$ species. The latter was shown to form *via* an ambient-temperature C–N cleavage involving unstable $Pd(OAc)_2(NHR_2)_2$ intermediates. Using pyridine as base eliminated this dealkylation and resulted in the exclusive formation of LPd(py) complexes in high yields. In total, seven novel Pd^{II} ABP complexes were prepared, exhibiting distorted square-planar geometries with the asymmetric ligand moieties orientated towards the metal centre. The air- and moisture-stable LPd(py) complexes were successfully employed as catalysts in two types of C–C coupling reactions. The Suzuki–Miyaura coupling of 4′-bromoacetophenone and phenylboronic acid reached high yields (up to 81%), while a scope of further alkyl bromides was also efficiently converted using low catalyst loadings (1 mol%) and mild temperatures (40 °C). Furthermore, a Pd–pyridine complex achieved high activity in the Mizoroki–Heck coupling of styrene and 4′-bromoacetophenone.

Received 9th September 2021,
Accepted 12th November 2021

DOI: 10.1039/d1dt03068j

rsc.li/dalton

Introduction

Amine bisphenolate (ABP) ligands are widely applied in homogeneous catalytic reactions due to their facile synthesis and versatile, easily tuneable properties.[1] Over the last few decades, a vast array of ABP metal complexes have been reported (Fig. 1, left), many of them serving as efficient catalysts in chemical processes, such as oxidations,[2] C–C coupling reactions,[3] as well as the polymerisation of cyclic esters and alkenes.[4,5] In these catalytic systems, the chelating ABP ligands provided remarkable stability *via* coordination to the metal centre in a tri- (O,N,O) or tetradentate (O,N,O,X) fashion. Moreover, the stereoelectronic effects of different substituents (on the phenolate moieties and on the pendant arm) were shown to subtly influence both the activity and selectivity of the catalysts, including enantioselective applications using chiral motifs.[6,7] As the synthesis of these ligands involves the Mannich condensation of primary amines, a particularly attractive strategy is the incorporation of inexpensive, naturally occurring chiral amino acid moieties into the ABP scaffold (Fig. 1, right). This may enable us to fine-tune the corresponding complexes stereo- and enantioselectivity as well as to influence their bioactivity. Surprisingly, amino acid-derived ABP ligands and their complexes are relatively underexplored; only a small range of metal complexes (including Be, Al, Fe and Co species) have been reported featuring achiral, glycine-based ligands.[8–20] Moreover, only a handful of examples exist with chiral analogues, such as alanine- and valine-derived ABP species.[21–23]

Complexes of Pd are exceptionally widely used in homogeneous catalysis, as they generally demonstrate high tolerance towards a wide range of substrates and impurities, as well as showing excellent reaction rates under relatively mild con-

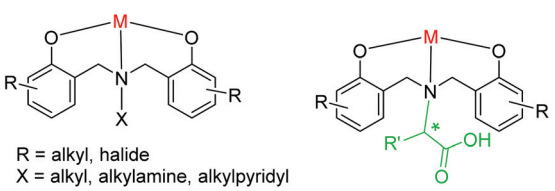

Fig. 1 General structure of amine bisphenolate complexes (left) and their amino acid derivatives (right).

Institute of Chemical Sciences, Heriot-Watt University, Edinburgh, EH14 4AS, UK. E-mail: r.mcintosh@hw.ac.uk

† Electronic supplementary information (ESI) available. CCDC 2070846, 2070847, 2070849–2070851, 2070853, 2063653, 2063654, 2060147, 2060195, 2060200 and 2060206. For ESI and crystallographic data in CIF or other electronic format see DOI: 10.1039/d1dt03068j

ditions. Common applications include Pd-catalysed C–C coupling; such as the Suzuki–Miyaura and the Mizoroki–Heck reactions, which have become indispensable tools in synthetic chemistry. In these processes, the Pd metal is most commonly stabilised with phosphine ligands; however, more recently phosphine-free catalyst systems have been gaining traction due to their increased air- and moisture-stability and cost-efficiency.[24,25] These alternative catalysts utilise NHC and other N-, O- or S-donor ligands, including amide, diamine bisphenolate, hydrazone, salen as well as water-soluble sulfosalan ligands.[26–34] Despite the popularity of ABP complexes across the board of catalytic processes (featuring an expansive array of transition metals), studies investigating these ligands' coordination to Pd remain scarce.[35] A handful of ABP ligands in combination with Pd precursors were reported to successfully catalyse the C–C coupling of phenylboronic acids and aryl bromides.[36–38] These systems are proposed to operate through the *in situ* formation of catalytically active Pd species, which are typically not isolated or characterised. Previous findings in this field suggest that the separation and fine-tuning of well-defined Pd complexes would provide a key opportunity to further optimise their catalytic activity and selectivity.

This work – building on our previous studies of amine bisphenolate complexes in catalysis – examines the incorporation of ester-protected amino acids into the ABP scaffold, generating a library of novel, chiral derivatives. We have thoroughly investigated the previously underexplored complexation of these ligands to Pd, which resulted in unique species with unprecedented coordination environments. Furthermore, the robust and well-defined Pd^{II} complexes obtained were successfully employed as catalysts in Suzuki–Miyaura and Mizoroki–Heck cross coupling reactions.

Results and discussion

Synthesis of ABP pro-ligands

Six ABP pro-ligands were synthesised through the double Mannich condensation of dialkyl phenols, formaldehyde and amino acid ethyl esters in water at 80 °C (Scheme 1). The application of ester-protected derivatives in place of the unprotected amino acids was found to provide significantly higher yields in comparison to our previously reported method and allowed for the facile purification of the obtained ABP pro-ligands.[39,40] The di-^{t}Bu-phenol derivatives (**L1–L3**) were obtained as white solids with moderate to good isolated yields of 32–72% after recrystallisation from dichloromethane and methanol. The dimethylphenol analogues (**L4–L6**) showed limited solubility in common organic solvents, which hampered their efficient recrystallisation and resulted in relatively lower yields (16–53%). Overall, a positive trend of yields was observed with decreasing bulk (H < Me < Bn) on the pendant arm of the ligands, possibly arising from the sterically more demanding alanine and phenylalanine moieties hindering the Mannich condensation reaction. The formation of the desired products was indicated by the appearance of diagnostic *N*-methylene resonances ($CDCl_3$ solvent, **L1**, δ = 3.69; **L2**, δ = 4.09; **L3**, δ = 4.11; **L4**, δ = 3.65; **L5**, δ = 4.00; **L6**, δ = 4.09) in the ^{1}H NMR spectra of the crude reaction mixtures. These pro-ligands are among the first examples of ABP derivatives featuring an ester-protected carboxylate pendant arm.[21,41]

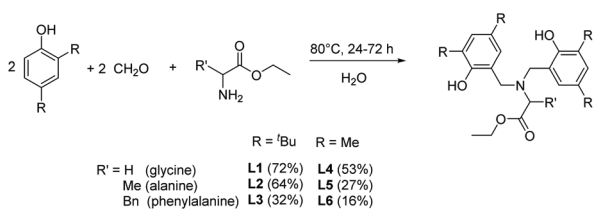

Scheme 1 Synthesis of amino acid-derived pro-ligands **L1–L6**.

The chiral ABP pro-ligands derived from L-alanine (**L2** and **L5**) and L-phenylalanine (**L3** and **L6**) were further examined to ensure enantiomeric purity. Polarimetry analysis of the di-^{t}Bu substituted **L2** and **L3** showed significant optical rotation values of $[\alpha]_D^{21.1} = -6.0$ (c 1.6, $CHCl_3$) and $[\alpha]_D^{21.5} = -13.0$ (c 1.6, $CHCl_3$), respectively, which suggested that these compounds had not fully racemised during the synthesis. Chiral HPLC studies of the dimethylphenol derivatives (**L5** and **L6**) allowed for the development of a suitable separation method (Fig. S22 and 23†). Use of a 1 M NaOH solution to liberate the amino acid ethyl ester starting material from the hydrochloride salt was found to result in significant racemisation, however, switching to a milder base ($NaHCO_3$) eliminated this problem affording an excellent enantiomer ratio (**L5** 97 : 3 e.r.). Notably, the HPLC separation of the di-^{t}Bu-substituted pro-ligands (**L2** and **L3**) was hampered by their extremely high solubility, which caused co-elution of the enantiomers in all hexane–isopropanol ratios of the solvent mixture. In addition, ^{1}H NMR studies of **L2** were also carried out in the presence of five equiv. of (*R*)-(−)-1-(9-anthryl)-2,2,2-trifluoroethanol shift reagent (Fig. S21†) to confirm the retention of chirality in di-^{t}Bu-phenol ABP derivatives. These experiments showed a diagnostic split of the *N*-methylene resonance ($CDCl_3$ solvent, δ = 4.09) for racemic **L2**. However, this shift was not detected in the pro-ligands synthesised from enantiomerically pure L-alanine, further corroborating the retention of chirality.

Synthesis of Pd complexes

To explore the coordination behaviour of the ABP ligands, complexation experiments were carried out using several Pd precursors, including $Pd(OAc)_2$, $PdCl_2$ and $Pd(NO_3)_2$. Initial attempts of mixing the pro-ligands with 1 equiv. of Pd precursor in common organic solvents were unsuccessful, including trials at elevated temperatures or in the presence of inorganic bases (KOH or NaH). Ultimately, the reaction of **L1** with Pd $(OAc)_2$ in the presence of 2 eq. of triethylamine (NEt_3) afforded a mixture of two complexes after stirring at ambient temperature for two hours in tetrahydrofuran (Scheme 2). An L1PdNEt_3 complex (**C1**) with triethylamine as ancillary ligand formed as minor component, while an unexpected L1Pd$NHEt_2$ complex (**C2**) was found to be the major product. The formation of

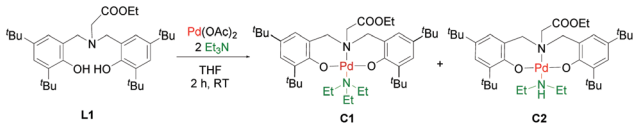

Scheme 2 Synthesis of Pd complexes **C1** and **C2**.

these species was indicated by a swift colour change from light orange (Pd precursor in solvent) to dark red after the first ten minutes of the reaction. The coordination of the ABP ligand to Pd was confirmed *via* the appearance of the *N*-methylene resonances as doublets (J = 12.4 Hz) in the ^{1}H NMR spectra, indicating that these protons had become diastereotopic upon complexation. The complexes were separated *via* column chromatography and further purified through recrystallisation from dichloromethane affording **C1** as red crystals and **C2** as dark orange crystals with yields of 14% and 35%, respectively. Full characterisation of these species was carried out including single crystal X-ray diffraction studies (*vide infra*) to highlight the complexes' unique molecular structure. To the best of our knowledge, these are the first examples of an ABP-type ligand coordinated to a Pd centre in a tridentate, O,N,O fashion. Complexes of ABP ligands with N-donor pendant arms have been previously reported to only partially coordinate to Pd (in O,N,N or N,N fashion).[35] Notably, this firm pincer-like chelation provided **C1** and **C2** with remarkable stability, including the air- and moisture-tolerant synthesis as well as remaining unchanged in solutions for up to four months. Purified samples of **C1** and **C2** also showed good thermal stability (up to 70 °C) both in $CDCl_3$ solutions and in neat form. However, heating the reaction mixture over 50 °C during the synthesis led to the rapid precipitation of Pd^0 black particles, indicating sensitivity towards acids and bases (AcOH and NEt_3) present prior to the purification, or the presence of less stable intermediates.

To investigate the C–N bond cleavage, which is concomitant with the formation of **C2**, we explored whether it was possible to directly convert an isolated sample of **C1** to **C2**. A wide range of reaction conditions was trialled including elevated temperatures (50 °C) or the addition of acids and bases (NEt_3, AcOH, NaOAc), but none of these attempts were fruitful. Alternative trialkylamine bases such as Pr_3N and Bu_3N showed similar behaviour, forming a mixture of $LPdNR_3$ and $LPdNHR_2$ complexes as indicated by the appearance of corresponding aromatic proton resonances ($CDCl_3$ solvent, δ = 6.76 and 6.83) in the ^{1}H NMR spectra of reaction mixtures and the isolation of a $PdNHPr_2$ complex (**C7**). Using Me_3N, an $LPdNMe_3$ complex (**C3**) was isolated as the sole product, indicating that this amine did not undergo dealkylation under the applied reaction conditions (THF, r.t., 24 h). However, SCXRD studies of **C3** showed partial occupancy on one of the *N*-methyl moieties, revealing that the corresponding $LPdNHMe_2$ complex is also present. This trend follows previous studies confirming that amines with a methylene (CH_2) group on the nitrogen undergo metal-catalysed C–N cleavage more readily, possibly *via* a β-hydrogen elimination process through imine and Pd–H species.[42,43] Notably, no complexation took place when carrying out the synthesis with triphenylamine under identical conditions, likely due to the steric hindrance caused by the bulky Ph groups, preventing the ABP ligand coordination. Variable temperature ^{1}H NMR experiments in THF-d_8 (from 20 °C to 50 °C) were carried out to better understand the generation of **C1** and **C2**. Acetaldehyde resonances ($CDCl_3$ solvent, δ = 9.20) detected prior to the appearance of resonances corresponding to **C2** suggested that the hydrolysis of Et_3N precedes the coordination of the ABP ligand (Scheme 3). Similar Pd-catalysed oxidative hydrolysis of tertiary amines, leading to aldehyde by-products through iminium ion and enamine intermediates, has been observed by Murahashi *et al.*, albeit using a heterogeneous Pd catalyst and harsher conditions (40 h, 200 °C).[44] The pathway depicted in Scheme 3 was further confirmed by the presence of resonances corresponding to $Pd(OAc)_2(NEt_3)_2$ and $Pd(OAc)_2(NHEt_3)_2$ complexes (dmso-d_6 solvent, δ = 1.65 and 1.55).[45] The latter species – formed through the coordination of hydrolysed $HNEt_2$ to $Pd(OAc)_2$ – was found to be thermally unstable, which accounts for the aforementioned decomposition to Pd^0 black particles, especially at temperatures above 40 °C.[46] These simple Pd $(OAc)_2(amine)_2$ complexes have been previously observed, as $Pd(OAc)_2/Et_3N$ catalyst systems are widely applied in the aerobic oxidation of alcohols, where the C–N cleavage forming $HNEt_2$ is considered an unfavourable catalyst degradation process.[47,48] Although the ratio of $Pd(OAc)_2(NHEt_3)_2$ could be reduced through limiting the excess of NEt_3 present in the reaction mixture, the dealkylation could not be completely excluded. Consequently, a mixture of **C1** and **C2** was formed under all reaction conditions tested and regardless of the order in which the reagents were added.

To investigate the coordination to Pd in the absence of amine hydrolysis side-reactions, further complexations of **L1–L3** were carried out using pyridine as the base. Upon addition of the reactants at ambient temperature, the immediate formation of a white precipitate was observed, which was isolated and identified as a $Pd(OAc)_2(pyridine)_2$ complex, structurally analogous to the trialkylamine derivatives observed with **C1** and **C2**.[45] Raising the temperature to 66 °C in THF solvent afforded the desired LPd(py) complexes **C4–C6** with decent

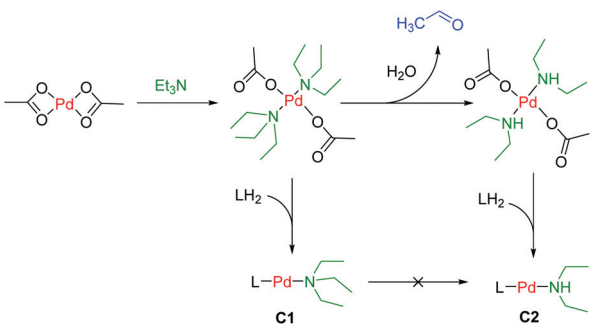

Scheme 3 Proposed pathway for the formation of **C1** and **C2**.

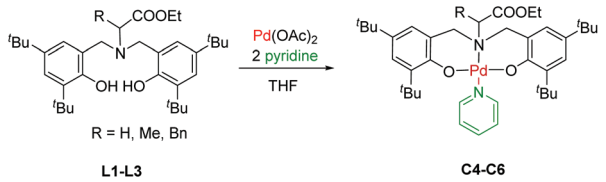

Scheme 4 Synthesis of Pd–pyridine complexes (**C4–C6**).

yields (22–55%). Notably, an extension of reaction time was required with increasing steric bulk on the amino acid moiety, with the glycine derivative (**C4**) reaching maximal conversion after 24 hours, the alanine derivative (**C5**) after 48 hours and the phenylalanine derivative (**C6**) after 72 hours (Scheme 4). The LPd(py) complexes – isostructural to the LPd(NR_3) analogues – formed as sole products allowing a simple purification *via* recrystallisation from acetonitrile to give **C4–C6** as deep red crystals.

Crystallography

Single crystals, suitable for X-ray diffraction studies, were grown *via* the slow evaporation of dichloromethane (**C1–C3**) or acetonitrile (**C4–C6**) solutions of the respective complexes. The crystallographic studies revealed that all six complexes exhibited a mononuclear structure, with the ABP ligand bonded to Pd in a tridentate fashion through the central nitrogen and the two phenolic oxygen atoms, which are *trans* to one another (Fig. 2–4). The fourth coordination site was occupied by the

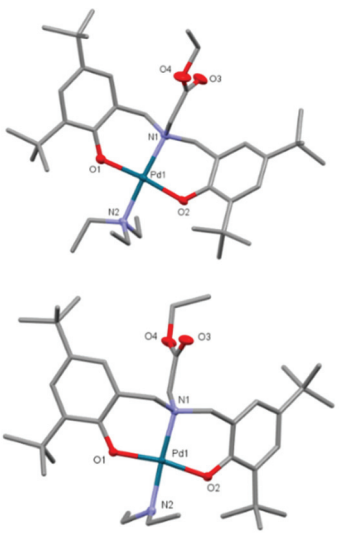

Fig. 2 Molecular structures of **C1** and **C2** with ellipsoids set at the 50% probability level. Hydrogen atoms have been omitted for clarity. Selected bond lengths for **C1** (Å): Pd1–O1 2.024(4), Pd1–N2 2.133(3), Pd1–O2 2.020(4), Pd1–N1 2.082(3). Selected bond angles for **C1** (°): O1–Pd1–N1 88.6(1), O1–Pd1–N2 93.5(1), O2–Pd1–O1 173.8(2), O2–Pd1–N1 86.0(1), O2–Pd1–N2 92.4(1), N2–Pd1–N1 169.6(1). Selected bond lengths for **C2** (Å): Pd1–O1 2.001(2), Pd1–N2 2.056(2), Pd1–O2 2.014(2), Pd1–N1 2.061(2). Selected bond angles for **C2** (°): O1–Pd1–N1 82.30(7), O1–Pd1–N2 95.08(7), O2–Pd1–O1 170.79(6), O2–Pd1–N1 88.49(7), O2–Pd1–N2 94.06(7), N2–Pd1–N1 173.20(8).

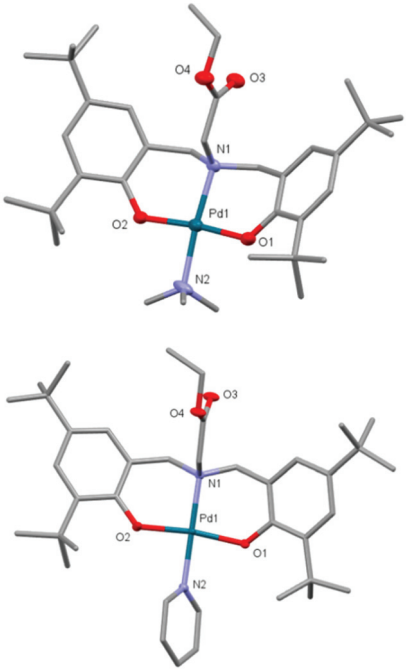

Fig. 3 Molecular structures of **C3** and **C4** with ellipsoids set at the 50% probability level. Hydrogen atoms have been omitted for clarity. Selected bond lengths for **C3** (Å): Pd1–O1 2.016(2), Pd1–N1 2.064(3), Pd1–O2 2.020(2), Pd1–N2 2.100(3). Selected bond angles for **C3** (°): O1–Pd1–N1 92.67(9), O1–Pd1–N2 85.7(1), O2–Pd1–O1 172.98(9), O2–Pd1–N1 93.71(9), O2–Pd1–N2 88.3(1), N2–Pd1–N1 172.6(1). Selected bond lengths for **C4** (Å): Pd1–O1 2.0002(9), Pd1–N1 2.046(1), Pd1–O2 1.9853(9), Pd1–N2 2.039(1). Selected bond angles for **C4** (°): O1–Pd1–N1 94.45(4), O1–Pd1–N2 85.84(4), O2–Pd1–O1 172.28(4), O2–Pd1–N1 93.12(4), O2–Pd1–N2 86.66(4), N2–Pd1–N1 177.81(4).

ancillary alkyl-amine or pyridine ligand. As generally expected for Pd^{II} complexes, slightly distorted square planar geometries were observed around the metal centre.[49] The four-coordinate geometry index (τ_4) ranged from 0.060 to 0.118 (where $\tau_4 = 0$ for perfectly square planar complexes and $\tau_4 = 1$ for perfectly tetrahedral complexes).[50] Notably, the Pd–pyridine complexes showed relatively lower τ_4 values (0.070 for **C4**, 0.074 for **C5** and 0.060 for **C6**) in comparison to the alkyl-amine-substituted analogues (0.118 for **C1**, 0.114 for **C2** and 0.102 for **C3**). This suggested that the more sterically demanding NMe_3, NEt_3 and $NHEt_2$ ancillary ligands create greater distortion than the planar and more compact pyridine. Likewise, the N1–Pd1–N2 axes involving the ancillary pyridine ligands (**C4–C6**) were nearly linear, ranging between 176.22(8)° and 177.81(4)°, while the Pd–amine complexes (**C1–C3**) featured more distorted axes of 169.64(1)°–173.20(1)°. The O1–Pd1–N1 and O2–Pd1–N2 angles fell between 82.34(9)° and 95.06(9)° – a significant deviation from the standard 90° value – indicating a degree of strain around the metal.[26] The O1–Pd1–O2 angles were found to be nearly linear ranging from 170.79(8)° to 174.46(6)°, while the dihedral angles between the planes of the two phenolate rings averaged around 130°. The Pd1–O1 and Pd1–O2 bond lengths [between 1.9853(9) Å and 2.024(4) Å] were close to one another and fall in line with values reported for other Pd–

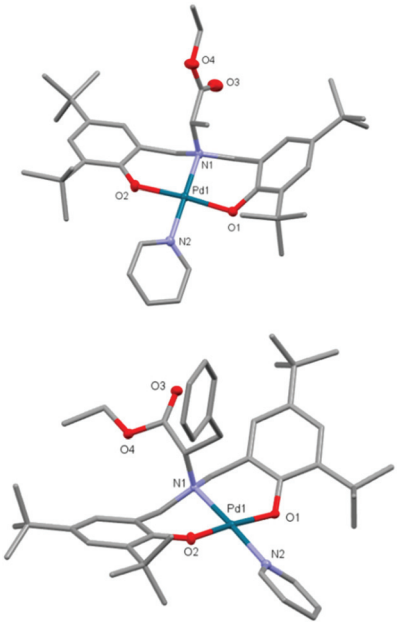

Fig. 4 Molecular structures of **C5** and **C6** with ellipsoids set at the 50% probability level. Hydrogen atoms and co-crystallised solvent have been omitted for clarity. Selected bond lengths for **C5** (Å): Pd1–O1 2.002(2), Pd1–N1 2.053(2), Pd1–O2 2.005(2), Pd1–N2 2.036(2). Selected bond angles for **C5** (°): O1–Pd1–N1 93.89(7), O1–Pd1–N2 86.57(7), O2–Pd1–O1 173.37(7), O2–Pd1–N1 92.47(7), O2–Pd1–N2 87.21(8), N2–Pd1–N1 176.22(8). Selected bond lengths for **C6** (Å): Pd1–O1 2.006(2), Pd1–N1 2.062(2), Pd1–O2 2.011(2), Pd1–N2 2.053(2). Selected bond angles for **C6** (°): O1–Pd1–N1 94.00(7), O1–Pd1–N2 86.84(7), O2–Pd1–O1 174.46 (6), O2–Pd1–N1 91.51(7), O2–Pd1–N2 87.68(7), N2–Pd1–N1 177.11(8).

phenolate complexes.[29,34,51] The Pd1–N1 and Pd1–N2 bond lengths ranging from 2.036(2) Å to 2.061(2) Å were similar for complexes containing planar pyridine and diethylamine ancillary ligands (**C2**, **C4–C6**). However, significantly longer Pd1–N2 bond lengths were observed for complexes containing sterically more demanding trialkylamine ancillary ligands [2.133(3) Å for **C1** and 2.100(3) Å **C3**]. The ester protected carboxylate groups were found not to be participating in the coordination to Pd and in fact pointing away from the Pd centre in these solid-state structures. The substituents (H, Me or Bn) on the ABP ligand pendant arm did not exhibit any significant influence on the coordination. In case of chiral complexes (**C5** and **C6**), the chiral methyl and benzyl moieties of the alanine and phenylalanine derivatives, respectively, were shown to bend near the metal centre, which is a promising feature for application in asymmetric catalysis. The molecular structures of all six ABP pro-ligands (**L1–L6**) were also determined using single crystal X-ray diffraction studies (Fig. S19 and S20†). The bond lengths and bond angles in these pro-ligands fall in line with previously reported ABP derivatives in the literature.[36]

Catalytic activity in C–C coupling

To gauge the efficiency of the obtained Pd^{II} ABP species in C–C cross coupling, the pyridine-derived complexes (**C4–C6**) were tested as catalysts in Suzuki–Miyaura reactions (Fig. S45†). The

Table 1 Optimisation of Suzuki–Miyaura reaction conditions

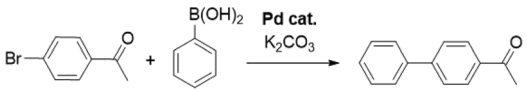

Entry	Catalyst	Solvent	T (°C)	Time (h)	Cat. load. (mol%)	Conv. (%)
1	**C4**	MeOH	40	3	1	37
2	**C4**	H_2O	40	3	1	<1
3	**C4**	Toluene	40	3	1	29
4	**C4**	DCM	40	3	1	28
5	**C4**	THF	40	3	1	5
6	**C4**	MeOH	r.t.	1	1	18
7	**C4**	MeOH	40	1	1	22
8	**C4**	MeOH	60	1	1	43
9	**C4**	MeOH	40	24	1	81
10	**C4**	MeOH	40	1	0.1	5
11	**C4**	MeOH	40	24	0.1	44
12	**C5**	MeOH	40	3	1	21
13	**C6**	MeOH	40	3	1	8
14	**C4**	MeOH	40	4	1	44
15	**C4** + Hg	MeOH	40	4	1	34

Conditions: 0.5 mmol 4′-bromoacetophenone, 0.75 mmol phenylboronic acid, 1 mmol K_2CO_3 in 10 ml solvent. Conversions determined *via* ^{1}H NMR integration against 1,3,5-trimethoxybenzene internal standard.

coupling of 4′-bromoacetophenone and phenylboronic acid using **C4** was chosen as the model reaction for initial optimisation (Table 1). Following literature precedents, K_2CO_3 was applied as an external base.[34,36] First, a range of different solvents was screened over a three hour reaction at 40 °C using 1 mol% catalyst. The highest conversion towards the desired 4-acetylbiphenyl product was achieved in methanol (37%, Table 1, entry 1), which is a typically preferred solvent for Pd catalysed Suzuki–Miyaura reactions using phosphine-free ligands.[24]

Catalyst **C4** also showed significant activity in dichloromethane and toluene (entries 3 and 4), while the conversion significantly dropped using THF (5%, entry 5). Only traces of the coupled product were observed when carrying out the reaction in water (entry 2), which was attributed to the extremely low solubility of the catalyst in this solvent. The optimisation of the reaction temperature showed that, predictably, a decrease from 40 °C to room temperature slightly lowered the conversion (from 22% to 18% after 1 h, entries 6 and 7). Remarkably, raising the temperature to 60 °C has doubled the rate of reaction (from 22% to 43%, entries 7 and 8), however, the precipitation of black particles was also observed, indicating limited thermal stability under these conditions. As Pd^0 nanoparticles are known to exhibit activity in Suzuki–Miyaura reactions, the temperature limit of 40 °C was chosen to minimise catalyst decomposition. The potential contribution of heterogeneous catalysis to the overall yields was further investigated (*vide infra*). Although lowering the catalyst loading from 1 mol% to 0.1 mol% (*cf.* entries 7 and 10) led to a significant drop in conversion from 22% to 5% after one hour at 40 °C, **C4** still showed activity after 24 hours reaching a conversion of

44% (entry 11). Importantly, control reactions applying the free pro-ligand **L1** or an '*in situ* complex' formed from **L1** and $Pd(OAc)_2$ did not yield the desired product in detectable quantities. Moreover, the presence of homo-coupled biaryl by-products was not observed *via* LC-MS analysis of the crude reaction mixtures. Under the established optimum conditions, the alanine- and phenylalanine-derived Pd ABP complexes were also tested (entries 12 and 13). Comparatively lower conversions of 21% and 8% were achieved, a trend reflecting the increasing steric bulk of the ABP ligand pendant arms on **C5** and **C6**, respectively.

A time-dependent study was carried out using catalyst **C4** under the optimised reaction conditions (Fig. 5). After a faster period in the initial 10 minutes, a linear reaction profile was observed in the first six hours, reaching 49% conversion. In later stages, the reaction gradually slowed down achieving 81% conversion after 24 hours (Table 1, entry 9), indicating that the catalyst remains active over an extended period. To examine the potential effect of heterogeneous Pd particles (formed *via* thermal decomposition) on the catalysis, 'mercury poisoning' control reactions were carried out using **C4** catalyst (Table 1, entries 14 and 15).[52] Under the optimised conditions (MeOH, 40 °C, 1 mol% catalyst loading) the formation of black particles was not visually observed, however, the conversion dropped from 44% to 34% in the presence of excess Hg^0. This may indicate that – while the majority of activity is derived from the homogeneous complex – an interplay of heterogeneous species cannot be excluded, especially at elevated temperatures.[53] The exact mechanism and the nature of 'true catalytic species' in Suzuki–Miyaura reactions using phosphine-free Pd^{II} complexes is heavily debated: along with Pd^0 intermediates formed *via* the disassociation of hemilable anionic ligands, the reaction was also proposed to proceed through pincer-stabilised Pd^{IV} species.[31,54–56]

Under the optimised conditions, the substrate scope of the Suzuki–Miyaura couplings using **C4** was extended to a small range of further aryl halides (Fig. 6). While bromo-4-nitrobenzene featuring a strongly electron withdrawing NO_2 group in *para* position to the bromine facilitated quantitative conversion, electron donating substituents such as NH_2 on 4-bromoaniline provided a lower yield of 68%. Reaction of *meta*- and *para*-substituted 4-bromo-2-fluoronitrobenzene reached 58% after 24 hours. Sterically more demanding substrates such as 1-bromo-2-methoxynaphthalene and 1-bromo-4-*tert*butylbenzene could also be converted with moderate yields of 21% and 11%, respectively. Couplings with less activated substrates such as *ortho*-, *meta*- and *para*-bromotoluene only provided traces of the desired product at 40 °C and would likely require harsher conditions. As an example for more challenging aryl chlorides, 4′-chloroacetophenone was also tested, providing only traces of the coupled product after 24 hours of reaction time.

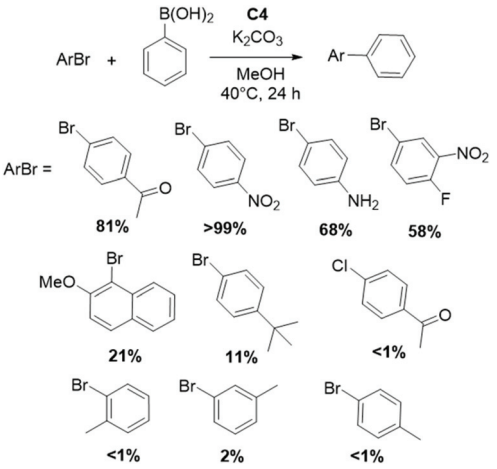

Fig. 6 Substrate scope of the Suzuki–Miyaura coupling reaction using **C4** as catalyst.

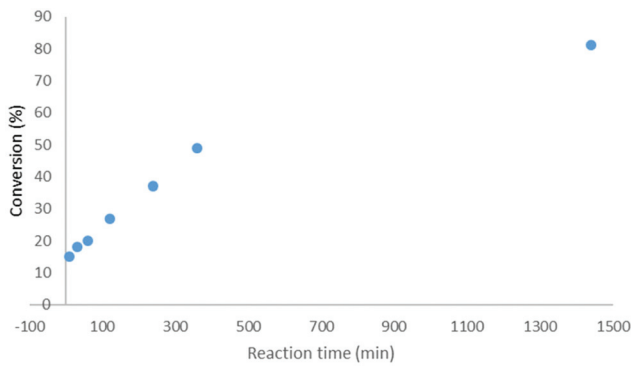

Fig. 5 Conversion *vs.* time of the Suzuki–Miyaura coupling using **C4** as catalyst.

The asymmetric Suzuki–Miyaura coupling of 1-napthaleneboronic acid and 1-bromo-2-methoxynaphthalene was attempted using the chiral **C5** catalyst (Scheme S1†). The established optimum conditions (MeOH, 40 °C) did not provide the desired axially chiral biaryl derivatives, even after prolonged reaction times (48 h). Increasing the temperature to 80 °C in dichloroethane solvent led to 53% conversion after 24 hours.[57] However, chiral HPLC studies of the product mixture showed that the two isomers formed in 1 : 1 ratio. Notably, the increased temperature facilitated the formation of Pd^0 black particles,[58] which have potentially contributed to the catalysis affording a racemic product mixture. The catalytic activity of **C4** was also probed in the Mizoroki–Heck reaction of 4′-bromoacetophenone and styrene following literature methods (Scheme S2†).[29] Using tetrabutylammonium bromide (TBAB) ionic solvent at 140 °C, the starting materials were quantitatively converted within 45 minutes towards the desired 4-acetylstilbene product (Fig. S46†). Similarly to the Suzuki–Miyaura reactions, the decomposition of the catalyst towards Pd^0 black particles was observed at 140 °C. Consequently, further mechanistic studies were hampered, as reducing the reaction temperature to 120 °C led to a dramatic decrease in activity, affording only traces of the product.

Conclusions

In conclusion, six amine bisphenol pro-ligands were synthesised featuring amino acid ethyl ester pendant arms. An optimised, milder synthetic method for the chiral L-alanine- and L-phenylalanine derivatives minimised racemisation and provided excellent enantiomer ratios. This novel ABP ligand family, incorporating inexpensive, naturally occurring amino acid moieties offers significant potential to coordinate to various metals and thus be utilised in a range of asymmetric catalytic processes. In the presence of amines, the ABP ligands were shown to form a series of air- and moisture-stable Pd^{II} complexes with an unprecedented tridentate O,N,O coordination mode. Using trialkylamines as ancillary ligands, a partial C–N cleavage reaction was observed under ambient conditions. Mechanistic studies of this phenomenon revealed that the dealkylation/hydrolysis occurred through $Pd(OAc)_2NR_3$ intermediates prior to the ligand coordination. Utilising pyridine in place of NR_3 was shown to prevent these competitive reactions and led to the selective formation of LPd(py)-type complexes with high yields. Single crystal X-ray diffraction studies of these species revealed that the chiral pendant arms are orientated towards the metal, a promising feature for selective catalysis. As a model reaction, the Pd complexes were employed in the Suzuki–Miyaura coupling of aryl bromides and phenylboronic acid, affording moderate conversions in methanol solvent at 40 °C. Moreover, the glycine-derived Pd complex **C4** also showed high activity in the Mizoroki–Heck coupling of styrene and 4-bromoacetophenone. While controlling the stereoselectivity of our catalyst system in asymmetric C–C coupling reactions remains a challenge, further optimisation of the ligand design and the reaction conditions is ongoing.

Experimental

General considerations

Starting materials were purchased and used as received from Merck, Acros and Fluorochem. Unless stated otherwise, experiments were carried out under ambient atmosphere. ^{1}H and ^{13}C NMR spectra were obtained on a Bruker AVIII spectrometer at 298 K at 300 MHz or 75 MHz. Chemical shifts (δ in ppm) were referenced to residual solvent ($CDCl_3$ at δ_H 7.26 ppm and δ_C 77.16 ppm). Electrospray ionisation (ESI) mass spectra were obtained on a Bruker micrOTOF spectrometer at the University of Edinburgh. Elemental analyses were carried out on an Exeter CE-440 Elemental Analyser. Enantiomer separation was achieved by chiral stationary phase HPLC (CSP-HPLC) with an Agilent Technologies 1120 Compact LC with a CHIRALPAK IB column. Optical rotation was measured on a Bellingham and Stanley ADP410 polarimeter.

General procedure for the synthesis of pro-ligands (L1–L6)

The amino acid ethyl ester hydrochloride (10 mmol, 1.40 g of glycine ethyl ester·HCl, 1.54 g of L-alanine ethyl ester·HCl or 2.30 g of L-phenylalanine ethyl ester·HCl) was dissolved in water (30 ml). $NaHCO_3$ (10 mmol, 0.84 g) was added and the solution was stirred for 20 minutes at r. t. To this solution, 20 mmol of phenol (4.13 g of 2,4-di-*tert*-butylphenol or 2.40 ml of 2,4-dimethylphenol) and formaldehyde (20 mmol, 1.5 ml of a 37 w% aqueous solution) were added and the mixture was heated to 80 °C for 24–72 hours. After cooling the mixture to 5 °C, an off-white precipitate was formed that was filtered and recrystallized from a mixture of DCM and methanol at r.t. to give the products as colourless crystals. Single crystals suitable for X-ray diffraction were obtained through the slow evaporation of DCM or $CDCl_3$ from the product solutions.

L1 Yield: 3.89 g (72%). ^{1}H NMR (300 MHz $CDCl_3$): 8.46 (s, 2H, O*H*), 7.24 (d, J = 2.4 Hz, 2H, Ar*H*), 6.88 (d, J = 2.4 Hz, 2H, Ar*H*), 4.27 (q, J = 7.1 Hz, 2H, CH_2CH$_3$), 3.69 (s, 4H, NCH_2), 3.35 (s, 2H, CH_2COOEt), 1.40 (s, 18H, CCH_3), 1.29 (t, J = 7.1 Hz, 3H, CH$_2$CH_3), 1.28 (s, 18H, CCH_3). ^{13}C NMR (75 MHz, $CDCl_3$): δ 173.0, 153.0, 141.1, 136.5, 125.1, 124.1, 120.5, 62.1, 57.5, 54.1, 35.2, 34.3, 31.8, 29.7, 14.2. HRMS (ESI): m/z $[M + H]^+$ found 540.4023, $[M + H]^+$ calculated 540.8010. Elemental analysis calculated for $C_{34}H_{53}NO_4$: C, 75.65; H, 9.90; N, 2.59. Found: C, 72.69; H, 9.59; N, 2.62. CCDC 2070846.†

L2 Yield: 3.54 g (64%). ^{1}H NMR (300 MHz $CDCl_3$): δ 8.67 (s, 2H, O*H*), 7.22 (d, J = 2.4 Hz, 2H, Ar*H*), 6.87 (d, J = 2.4 Hz, 2H, Ar*H*), 4.27 (qd, J = 7.1, 1.9 Hz, 2H, CH_2CH$_3$), 4.09 (d, J = 13.4 Hz, 2H, NCH_2), 3.75 (q, J = 7.2 Hz, 1H, NC*H*CH$_3$), 3.35 (d, J = 13.5 Hz, 2H, NCH_2), 1.39 (s, 18H, CCH_3), 1.37 (d, J = 6.6, 3H, NCHCH_3), 1.30 (t, J = 7.1 Hz, 3H, CH$_2$CH_3), 1.27 (s, 18H, CCH_3). ^{13}C NMR (75 MHz, $CDCl_3$): δ 175.4, 153.2, 140.9, 136.4, 125.2, 123.9, 120.4, 62.2, 55.8, 53.1, 35.1, 34.2, 31.8, 31.0, 29.6, 14.2. HRMS (ESI): m/z $[M + H]^+$ found 555.4282, $[M + H]^+$ calculated 554.8280. Elemental analysis calculated for $C_{35}H_{55}NO_4$: C, 75.9; H, 10.01; N, 2.53. Found: C, 75.99; H, 10.16; N, 2.66. $[\alpha]_D^{21.1}$ = −6.0 (c 1.6, $CHCl_3$). CCDC 2070847.†

L3 Yield: 1.93 g (32%). ^{1}H NMR (300 MHz $CDCl_3$): δ 8.30 (s, 2H, O*H*), 7.36–7.27 (m, 2H, Ar*H*), 7.25–7.16 (m, 3H, Ar*H*), 7.22 (d, J = 2.3 Hz, 2H, Ar*H*) 6.81 (d, J = 2.4 Hz, 2H, Ar*H*), 4.28–4.18 (m, 2H, CH_2CH$_3$), 4.11 (d, J = 13.4 Hz, 2H, NCH_2), 3.95 (dd, J = 7.6, 6.2 Hz, 1H, NC*H*CH$_2$Ph), 3.50 (d, J = 13.4 Hz, 2H, NCH_2), 3.31–3.04 (m, 2H, NCHCH_2Ph), 1.39 (s, 18H, CCH_3), 1.28 (s, 18H, CCH_3), 1.23 (t, J = 7.1 Hz, 3H, CH$_2$CH_3). ^{13}C NMR (75 MHz, $CDCl_3$): δ 174.5, 153.0, 141.1, 138.6, 136.4, 129.4, 128.7, 126.8, 125.6, 124.0, 120.5, 62.1, 61.9, 53.3, 35.1, 34.3, 32.4, 31.8, 29.7, 14.1. HRMS (ESI): m/z $[M + H]^+$ found 630.4499, $[M + H]^+$ calculated 630.4517. Elemental analysis calculated for $C_{41}H_{59}NO_4$: C, 78.18; H, 9.44; N, 2.22. Found: C, 78.00; H, 9.54; N, 2.40. $[\alpha]_D^{21.5}$ = −13.0 (c 1.6, $CHCl_3$). CCDC 2070849.†

L4 Yield: 1.97 g (53%). ^{1}H NMR (300 MHz, $CDCl_3$): δ 8.27 (s, 2H, O*H*), 6.87 (s, 2H, Ar*H*), 6.66 (s, 2H, Ar*H*), 4.24 (q, J = 7.2 Hz, 2H, CH_2CH$_3$), 3.65 (s, 4H, NCH_2), 3.30 (s, 2H, CH_2COOEt), 2.21 (d, J = 4.6 Hz, 12H, ArCH_3), 1.27 (t, J = 7.2 Hz, 3H, CH$_2$CH_3). ^{13}C NMR (75 MHz, $CDCl_3$): δ 173.1, 152.4, 131.8, 128.5, 128.2, 125.6, 120.3, 62.1, 57.0, 54.0, 20.5, 16.1, 14.2, 8.3. HRMS (ESI): m/z $[M + H]^+$ found 372.2098, $[M + H]^+$ calculated 372.2097. CCDC 2070850.†

L5 Yield: 1.04 g (27%). ^{1}H NMR (300 MHz $CDCl_3$): δ 8.53 (s, 2H, O*H*), 6.87 (s, 2H, Ar*H*), 6.66 (s, 2H, Ar*H*), 4.32–4.20 (m, 2H, CH_2CH_3), 4.00 (d, J = 13.4 Hz, 2H, NCH_2), 3.70 (q, J = 7.2 Hz, 1H, $NCHCH_3$), 3.30 (d, J = 13.4 Hz, 2H, NCH_2), 2.20 (d, J = 3.4 Hz, 12H, $ArCH_3$), 1.36 (d, J = 7.3, 3H, $NCHCH_3$), 1.28 (t, J = 7.2 Hz, 3H, CH_2CH_3). ^{13}C NMR (75 MHz, $CDCl_3$): δ 175.7, 152.5, 131.6, 128.6, 128.03, 125.6, 120.3, 62.2, 55.9, 52.6, 20.5, 16.1, 14.2, 8.3. HRMS (ESI): m/z $[M]^+$ found 385.2231, $[M]^+$ calculated 385.2253. $[\alpha]_D^{21.2}$ = +4.0 (c1, $CHCl_3$). 97 : 3 e.r.; HPLC (CHIRALPAK IA, hexane/2-propanol: 95/5, flow rate: 1.0 mL min^{-1}, detection UV 215 nm, 25 °C) t_R of major isomer: 5.87 min, t_R of minor isomer: 6.72 min. CCDC 2070851.†

L6 Yield: 0.73 g (16%). ^{1}H NMR (300 MHz $CDCl_3$): δ 8.15 (s, 2H, O*H*), 7.33–7.14 (m, 5H, Ar*H*), 6.86 (d, J = 1.3 Hz, 2H, Ar*H*) 6.53 (d, J = 1.7 Hz, 2H, Ar*H*), 4.29–4.12 (m, 2H, CH_2CH_3), 4.03 (d, J = 13.3 Hz, 2H, NCH_2), 3.90 (t, J = 6.9 Hz, 1H, $NCHCH_2Ph$), 3.48 (d, J = 13.4 Hz, 2H, NCH_2), 3.26–3.08 (m, 2H, $NCHCH_2Ph$), 2.19 (s, 12H, $ArCH_3$), 1.21 (t, J = 7.1 Hz, 3H, CH_2CH_3). ^{13}C NMR (75.5 MHz, $CDCl_3$): 174.3, 152.2, 138.5, 131.6, 129.4, 129.0, 128.7, 128.1, 126.8, 125.4, 120.4, 62.2, 62.1, 53.0, 32.7, 20.5, 16.1, 14.1. HRMS (ESI): m/z $[M + H]^+$ found 462.2604, $[M + H]^+$ calculated 462.2566. $[\alpha]_D^{21.4}$ = +2.0 (c2, $CHCl_3$). CCDC 2070853.†

General procedure for the synthesis of Pd complexes (C1–C7)

The ABP pro-ligand (0.5 mmol, 0.27 g of **L1**, 0.28 g of **L2** or 0.32 g of **L3**) was dissolved in THF (20 ml). $Pd(OAc)_2$ (0.5 mmol, 0.11 g) and the appropriate amine (1 mmol, 0.14 ml of Et_3N, 0.19 ml of Pr_3N, 0.24 ml of Bu_3N, 0.08 ml of pyridine or 1 ml of a Me_3N 1 M solution in THF) were added and the mixture was stirred for the appropriate reaction time (2 to 36 hours) at r. t. followed by a colour change from orange to dark red. Volatiles were removed *in vacuo* and the product was recrystallised from dichloromethane. Single crystals suitable for X-ray diffraction analysis were obtained through the slow evaporation of DCM or acetonitrile.

C1 Yield: 0.052 g (14%). ^{1}H NMR (300 MHz $CDCl_3$): δ 7.15 (d, J = 2.7 Hz, 2H, Ar*H*), 6.74 (d, J = 2.7 Hz, 2H, Ar*H*), 5.13 (d, J = 12.2 Hz, 2H, NCH_2), 3.97 (q, J = 6.7 Hz, 2H, OCH_2CH_3), 3.96 (d, J = 13.3 Hz, 2H, NCH_2), 3.25 (s, 2H, CH_2COOEt), 2.79 (q, J = 7.2 Hz, 6H, NCH_2CH_3), 1.55 (t, J = 6.7 Hz, 9H, NCH_2CH_3), 1.38 (s, 18H, CCH_3), 1.21 (s, 18H, CCH_3), 1.11 (t, J = 7.1 Hz, 3H, OCH_2CH_3). ^{13}C NMR (75 MHz, $CDCl_3$): δ 166.4, 160.0, 136.7, 135.7, 125.4, 125.0, 120.8, 60.7, 60.6, 47.1, 35.1, 33.9, 31.8, 29.7, 22.8, 14.3, 10.7. HRMS (ESI): m/z $[M + H]^+$ found 745.4149, $[M + H]^+$ calculated 745.4130. CCDC 2063653.†

C2 Yield: 0.125 g (35%). ^{1}H NMR (300 MHz $CDCl_3$): δ 7.15 (d, J = 2.7 Hz, 2H, Ar*H*), 6.76 (d, J = 2.6 Hz, 2H, Ar*H*), 4.89 (d, J = 12.4 Hz, 2H, NCH_2), 4.02 (q, J = 7.1 Hz, 2H, OCH_2CH_3), 4.02 (d, J = 12.4 Hz, 2H, NCH_2), 3.49 (s, 2H, CH_2COOEt), 3.16–3.05 (m, 2H, NCH_2CH_3), 2.82–2.63 (m, 1H, N*H*), 2.63–2.47 (m, 2H, NCH_2CH_3), 1.69 (t, J = 7.2 Hz, 6H, NCH_2CH_3), 1.37 (s, 18H, CCH_3), 1.22 (s, 18H, CCH_3), 1.14 (t, J = 7.1 Hz, 3H, OCH_2CH_3). ^{13}C NMR (75 MHz, $CDCl_3$): 166.5, 160.8, 136.6, 135.8, 125.7, 124.9, 120.8, 60.6, 60.1, 51.1, 47.1, 35.3, 33.9, 31.8, 29.9, 15.3, 14.3. HRMS (ESI): m/z $[M + H]^+$ found 717.3814; $[M + H]^+$ calculated 717.3440. Elemental analysis calculated for $C_{38}H_{62}N_2O_4Pd$: C, 63.63; H, 8.71; N, 3.91. Found: C, 62.09; H, 8.74; N, 4.20. CCDC 2063654.†

C3 Yield: 0.073 g (21%). ^{1}H NMR (300 MHz $CDCl_3$): δ 7.14 (d, J = 2.7 Hz, 2H, Ar*H*), 6.72 (d, J = 2.7 Hz, 2H, Ar*H*), 5.11 (d, J = 12.2 Hz, 2H, NCH_2), 3.95 (q, J = 7.2 Hz, 2H, CH_2CH_3), 3.94 (d, J = 12.5 Hz, 2H, NCH_2), 3.18 (s, 2H, CH_2COOEt), 2.60 (s, 9H, NCH_3), 1.40 (s, 18H, CCH_3), 1.20 (s, 18H, CCH_3), 1.09 (t, J = 7.1 Hz, 3H, CH_2CH_3). ^{13}C NMR (75 MHz, $CDCl_3$): δ 166.4, 160.2, 136.9, 136.1, 125.4, 124.8, 121.4, 60.6, 52.5, 49.7, 35.3, 34.0, 31.8, 29.8, 25.3, 14.2. HRMS (ESI): m/z $[M]^+$ found 703.3676, $[M]^+$ calculated 703.3663. CCDC 2060147.†

C4 Yield: 0.20 g (55%). ^{1}H NMR (300 MHz $CDCl_3$): δ 9.01–8.92 (m, 2H, py*H*), 7.88–7.79 (m, 1H, py*H*), 7.43–7.36 (m, 2H, py*H*), 7.14 (d, J = 2.6 Hz, 2H, Ar*H*), 6.80 (d, J = 2.6 Hz, 2H, Ar*H*), 4.96 (d, J = 12.4 Hz, 2H, NCH_2), 4.07 (d, J = 12.5 Hz, 2H, NCH_2), 4.03 (q, J = 7.1 Hz, 2H, CH_2CH_3), 3.49 (s, 2H, CH_2COOEt), 1.27 (s, 18H, CCH_3), 1.23 (s, 18H, CCH_3), 1.15 (t, J = 7.2 Hz, 3H, CH_2CH_3). ^{13}C NMR (75 MHz, $CDCl_3$): δ 166.5, 160.9, 151.1, 138.5, 137.4, 136.5, 125.3, 124.7, 123.9, 121.8, 60.7, 60.3, 50.1, 35.2, 34.0, 31.8, 29.5, 14.3. HRMS (ESI): m/z $[M + H]^+$ found 722.3348, $[M + H]^+$ calculated 722.3275. Elemental analysis calculated for $C_{39}H_{56}N_2O_4Pd$: C, 64.76; H, 7.80; N, 3.87. Found: C, 65.64; H, 8.07; N, 3.87. CCDC 2060195.†

C5 Yield: 0.09 g (24%). ^{1}H NMR (300 MHz $CDCl_3$): δ 9.00–8.94 (m, 2H, py*H*), 7.84 (tt, J = 7.7, 1.6 Hz, 1H, py*H*), 7.43–7.36 (m, 2H, py*H*), 7.12 (d, J = 2.6 Hz, 2H, Ar*H*), 6.81 (d, J = 2.3 Hz, 2H, Ar*H*), 5.23 (d, J = 13.2 Hz, 1H, NCH_2), 4.84 (d, J = 12.6 Hz, 1H, NCH_2), 4.11–3.97 (m, 2H, CH_2CH_3), 3.93 (d, J = 12.7 Hz, 1H, NCH_2), 3.91 (d, J = 13.4 Hz, 1H, NCH_2), 3.66 (q, J = 7.3 Hz, 1H, $NCHCH_3$), 1.63 (d, J = 7.6 Hz, 3H, $NCHCH_3$), 1.29 (s, 9H, CCH_3), 1.26 (s, 9H, CCH_3), 1.25 (s, 9H, CCH_3), 1.22 (t, J = 7.1 Hz, 3H, CH_2CH_3), 1.21 (s, 9H, CCH_3). ^{13}C NMR (101 MHz, $CDCl_3$) δ 169.2, 161.9, 160.7, 151.2, 138.4, 137.4, 136.9, 136.9, 135.7, 125.7, 125.1, 124.6, 124.4, 123.8, 123.6, 120.5, 63.1, 60.9, 59.9, 58.9, 35.2, 35.0, 34.1, 34.0, 31.9, 31.8, 29.6, 29.4, 16.3, 14.3. HRMS (ESI): m/z $[M + H]^+$ found 737.3532, $[M + H]^+$ calculated 737.3519. Elemental analysis calculated for $C_{40}H_{58}N_2O_4Pd$: C, 65.16; H, 7.93; N, 3.80. Found: C, 66.69; H, 8.41; N, 4.29. CCDC 2060200.†

C6 Yield: 0.09 g (22%). ^{1}H NMR (300 MHz $CDCl_3$): δ 9.00–8.87 (m, 2H, pyr*H*), 7.85 (tt, J = 7.6, 1.6 Hz, 1H, pyr*H*), 7.44–7.37 (m, 2H, pyr*H*), 7.15 (d, J = 2.6 Hz, 1H, Ar*H*), 7.12–7.02 (m, 7H, Ar*H*), 6.79 (d, J = 2.5 Hz, 1H, Ar*H*), 5.44 (d, J = 13.8 Hz, 1H, NCH_2), 4.56 (d, J = 12.0 Hz, 1H, NCH_2), 4.44 (d, J = 13.3 Hz, 1H, NCH_2), 3.95 (q, J = 14.0, 7.0 Hz, 2H, CH_2CH_3), 3.90 (d, J = 12.5 Hz, 1H, NCH_2), 3.87–3.80 (m, 2H, CH_2Ph), 2.79 (dd, J = 13.4, 11.4 Hz, 1H, $CHCOOEt$), 1.33 (s, 9H, CCH_3), 1.32 (s, 9H, CCH_3), 1.22 (s, 9H, CCH_3), 1.14 (s, 9H, CCH_3), 1.07 (t, J = 7.1 Hz, 3H, CH_2CH_3). ^{13}C NMR (75 MHz, $CDCl_3$): δ 168.1, 162.5, 160.1, 151.3, 150.0, 138.9, 138.5, 137.9, 137.4, 137.1, 135.7, 129.7, 128.2, 126.4, 125.8, 125.6, 124.6, 124.4, 124.0, 119.7, 67.0, 64.8, 60.9, 59.9, 38.3, 35.4, 34.9, 34.2, 33.9, 31.9, 31.9, 29.8, 29.3, 14.2. HRMS (ESI): m/z $[M + H]^+$ found 813.3832, $[M + H]^+$ calculated 813.3834. Elemental analysis calculated for $C_{46}H_{62}N_2O_4Pd$: C, 67.92; H, 7.68; N, 3.44. Found: C, 67.88; H, 7.74; N, 3.57. CCDC 2060206.†

C7 Yield: 0.04 g (10%). ^{1}H NMR (300 MHz, $CDCl_3$) δ 7.16 (d, J = 2.7 Hz, 2H, Ar*H*), 6.76 (d, J = 2.6 Hz, 2H, Ar*H*), 4.88 (d, J = 12.4 Hz, 2H, NCH_2), 4.02 (q, J = 13.4, 7.9 Hz, 2H, OCH_2CH$_3$), 4.00 (d, J = 12.6 Hz, 2H, NCH_2), 3.48 (s, 2H, CH_2COOEt), 3.11–3.01 (m, 2H,), 2.87 (s, 1H, N*H*), 2.51–2.39 (m, J = 6.3 Hz, 4H, CH_2CH$_2$CH$_3$), 2.09–2.01 (m, 4H, CH$_2$CH_2CH$_3$), 1.38 (s, 18H, CCH_3), 1.22 (s, 18H, CCH_3), 1.14 (t, J = 7.1 Hz, 3H, OCH$_2$CH_3), 1.01 (t, J = 7.2 Hz, 6H, CH$_2$CH$_2$CH_3). ^{13}C NMR (75 MHz, $CDCl_3$) δ 173.1, 152.6, 141.5, 136.2, 125.2, 123.8, 121.5, 61.3, 57.9, 50.6, 35.0, 34.3, 32.4, 31.8, 29.8, 14.2. HRMS (ESI): m/z $[M + H]^+$ found 745.4140; $[M + H]^+$ calculated 745.41329.

General procedure for Suzuki–Miyaura reactions

In a round bottom flask equipped with a magnetic stirring bar, Pd catalyst (0.005 mmol, 0.0036 g of **C4**), aryl halide (100 eq., 0.5 mmol, 0.100 g of 4′-bromoacetophenone), phenylboronic acid (150 eq., 0.75 mmol, 0.091 g), K_2CO_3 (200 eq., 1 mmol, 0.138 g) and 1,3,5-trimethoxybenzene (50 eq., 0.25 mmol, 0.042 g) were dissolved in methanol (10 ml). After stirring at 40 °C for the appropriate reaction time, the crude reaction mixture was diluted with water (10 ml) and extracted with diethyl ether (3 × 10 ml). The combined organic layers were dried over $MgSO_4$ and filtered, solvents were evaporated *in vacuo*. Conversion was determined *via* ^{1}H NMR spectroscopy against the 1,3,5-trimethoxybenzene internal standard.

General procedure for Mizoroki–Heck reactions

In a scintillation vial equipped with a magnetic stirring bar, Pd catalyst (0.005 mmol, 0.0036 g of **C4**), 4′-bromoacetophenone (200 eq., 1 mmol, 0.200 g), styrene (280 eq., 1.4 mmol, 0.146 g), NaOAc (220 eq., 1.1 mmol, 0.090 g), 1,3,5-trimethoxybenzene (50 eq., 0.25 mmol, 0.042 g) and tetrabutylammonium bromide ionic solvent (2.0 g) were added. The vial was closed with a screw cap and the mixture was melted, then heated to 120 °C for the appropriate reaction time. The crude reaction mixture was cooled to ambient temperature, dissolved in water (10 ml) and extracted with diethyl ether (3 × 10 ml). The combined organic layers were dried over $MgSO_4$ and filtered, solvents were evaporated *in vacuo*. Conversion was determined *via* ^{1}H NMR spectroscopy against the 1,3,5-trimethoxybenzene internal standard.

Crystallography

Single crystal X-ray diffraction data was collected on a Bruker D8 Venture diffractometer, with Mo-K_α (λ = 0.7107 Å) or Cu-K_α (λ = 1.5418 Å) radiation. The structures were solved by direct methods using SHELXS or intrinsic phasing SHELXT[59] and refined by full-matrix least-squares on F^2 using SHELXL interfaced through Olex2.[60,61] Molecular graphics for all structures were generated using Mercury.[62]

Conflicts of interest

There are no conflicts to declare.

Acknowledgements

This research was funded by EPSRC grants EP/N509474/1 and EP/S005781/1. The authors thank Dr Ai-Lan Lee, Dr Claire J. C. Lamb and Dr Jeff Y. F. Wong for their help with chiral HPLC and polarimetry studies, as well as Dr Graeme Barker and Dr David Ellis for their assistance with the NMR shift reagent studies.

Notes and references

1 O. Wichmann, R. Sillanpää and A. Lehtonen, *Coord. Chem. Rev.*, 2012, **256**, 371–392.
2 Y.-L. Wong, L. H. Tong, J. R. Dilworth, D. K. P. Ng and H. K. Lee, *Dalton Trans.*, 2010, **39**, 4602–4611.
3 R. R. Chowdhury, A. K. Crane, C. Fowler, P. Kwong and C. M. Kozak, *Chem. Commun.*, 2008, 94–96.
4 E. Y. Tshuva, S. Groysman, I. Goldberg, M. Kol and Z. Goldschmidt, *Organometallics*, 2002, **21**, 662–670.
5 J.-F. Carpentier, *Organometallics*, 2015, **34**, 4175–4189.
6 A. Amgoune, C. M. Thomas, S. Ilinca, T. Roisnel and J.-F. Carpentier, *Angew. Chem., Int. Ed.*, 2006, **45**, 2782–2784.
7 J.-B. Zhu and E. Y.-X. Chen, *Angew. Chem., Int. Ed.*, 2019, **58**, 1178–1182.
8 Y.-L. Duan, J.-X. He, W. Wang, J.-J. Zhou, Y. Huang and Y. Yang, *Dalton Trans.*, 2016, **45**, 10807–10820.
9 T. Heikkilä, R. Sillanpää and A. Lehtonen, *J. Coord. Chem.*, 2014, **67**, 1863–1872.
10 M. M. Hänninen, A. Peuronen, P. Damlin, V. Tyystjärvi, H. Kivelä and A. Lehtonen, *Dalton Trans.*, 2014, **43**, 14022–14028.
11 S. Saha, R. Majumdar, R. R. Dighe and A. R. Chakravarty, *Metallomics*, 2010, **2**, 754–765.
12 E. Safaei, H. Sheykhi, A. Wojtczak, Z. Jagličić and A. Kozakiewicz, *Polyhedron*, 2011, **30**, 1219–1224.
13 T. Weyhermüller, R. Wagner and P. Chaudhuri, *Eur. J. Inorg. Chem.*, 2011, **2011**, 2547–2557.
14 M. Roy, S. Saha, A. K. Patra, M. Nethaji and A. R. Chakravarty, *Inorg. Chem.*, 2007, **46**, 4368–4370.
15 O. Raymond, W. Henderson, P. J. Brothers and P. G. Plieger, *Eur. J. Inorg. Chem.*, 2018, **2018**, 1120–1130.
16 S. Indira, G. Vinoth, M. Bharathi, S. Bharathi, A. Kalilur Rahiman and K. Shanmuga Bharathi, *Inorg. Chim. Acta*, 2019, **495**, 118988.
17 Z. Taheri, B. Ghanbari and H. Hajibabaei, *Chem. Pap.*, 2014, **68**, 989–994.
18 A. S. Ceccato, A. Neves, M. A. de Brito, S. M. Drechsel, A. S. Mangrich, R. Werner, W. Haase and A. J. Bortoluzzi, *Dalton Trans.*, 2000, 1573–1577.
19 M. S. Shongwe, C. H. Kaschula, M. S. Adsetts, E. W. Ainscough, A. M. Brodie and M. J. Morris, *Inorg. Chem.*, 2005, **44**, 3070–3079.
20 J. Wilson, *Aust. J. Chem.*, 1990, **43**, 1283–1289.
21 A. Rajput, A. Kumar, A. Sengupta, P. Tyagi and H. Arora, *New J. Chem.*, 2018, **42**, 12621–12631.

22 Y. Xie, P.-W. Sun, Y. Li, S. Wang, M. Ye and Z. Li, *Angew. Chem., Int. Ed.*, 2019, **58**, 7097–7101.
23 H.-G. Fu, Z.-W. Li, X.-X. Hu, S.-Y. Si, X.-F. You, S. Tang, Y.-X. Wang and D.-Q. Song, *Molecules*, 2019, **24**, 548.
24 L. K. Mannepalli, C. Gadipelly, G. Deshmukh, P. Likhar and S. Pottabathula, *Bull. Chem. Soc. Jpn.*, 2020, **93**, 355–372.
25 W.-J. Jin, L.-Q. Ding, Z. Chu, L.-L. Chen, X.-Q. Lü, X.-Y. Zheng, J.-R. Song and D.-D. Fan, *J. Mol. Catal. A: Chem.*, 2011, **337**, 25–32.
26 S. Kumari, B. Das and S. Ray, *Dalton Trans.*, 2019, 15942–15954.
27 S. Bunda, A. Udvardy, K. Voronova and F. Joó, *J. Org. Chem.*, 2018, **83**, 15486–15492.
28 A. V. Kletskov, N. A. Bumagin, S. K. Petkevich, E. A. Dikusar, A. S. Lyakhov, L. S. Ivashkevich, I. A. Kolesnik and V. I. Potkin, *Inorg. Chem.*, 2020, **59**, 10384–10388.
29 L.-C. Liu, Y.-H. Tzeng, C.-H. Hung and H. M. Lee, *Eur. J. Inorg. Chem.*, 2020, 3601–3611.
30 A. Gogoi, A. Dewan, G. Borah and U. Bora, *New J. Chem.*, 2015, **39**, 3341–3344.
31 V. Arumugam, W. Kaminsky, N. S. P. Bhuvanesh and D. Nallasamy, *RSC Adv.*, 2015, **5**, 59428–59436.
32 A. R. Chaudhary and A. V. Bedekar, *Appl. Organomet. Chem.*, 2012, **26**, 430–437.
33 E. G. Bowes, G. M. Lee, C. M. Vogels, A. Decken and S. A. Westcott, *Inorg. Chim. Acta*, 2011, **377**, 84–90.
34 S. Mohanty, D. Suresh, M. S. Balakrishna and J. T. Mague, *J. Organomet. Chem.*, 2009, **694**, 2114–2121.
35 B. J. Graziano, E. M. Collins, N. C. McCutcheon, C. L. Griffith, N. M. Braunscheidel, T. M. Perrine and B. M. Wile, *Inorg. Chim. Acta*, 2019, **484**, 185–196.
36 A. K. Bowser, A. M. Anderson-Wile, D. H. Johnston and B. M. Wile, *Appl. Organomet. Chem.*, 2016, **30**, 32–39.
37 S. Mohanty, D. Suresh, M. S. Balakrishna and J. T. Mague, *Tetrahedron*, 2008, **64**, 240–247.
38 Z. Zhou, M. Liu, X. Wu, H. Yu, G. Xu and Y. Xie, *Appl. Organomet. Chem.*, 2013, **27**, 562–569.
39 J.-M. E. P. Cols, C. E. Taylor, K. J. Gagnon, S. J. Teat and R. D. McIntosh, *Dalton Trans.*, 2016, **45**, 17729–17738.
40 J.-M. E. P. Cols, V. G. Hill, S. K. Williams and R. D. McIntosh, *Dalton Trans.*, 2018, **47**, 10626–10635.
41 Y. Li, D. Yu, Z. Dai, J. Zhang, Y. Shao, N. Tang and J. Wu, *Dalton Trans.*, 2015, **44**, 5692–5702.
42 K. Ouyang, W. Hao, W.-X. Zhang and Z. Xi, *Chem. Rev.*, 2015, **115**, 12045–12090.
43 A. S. Guram, R. A. Rennels and S. L. Buchwald, *Angew. Chem., Int. Ed. Engl.*, 1995, **34**, 1348–1350.
44 S. Murahashi and T. Watanabe, *J. Am. Chem. Soc.*, 1979, **101**, 7429–7430.
45 S. V. Kravtsova, I. P. Romm, A. I. Stash and V. K. Belsky, *Acta Crystallogr., Sect. C: Cryst. Struct. Commun.*, 1996, **52**, 2201–2204.
46 J. Sanmartín-Matalobos, C. González-Bello, L. Briones-Miguéns, M. Fondo and A. M. García-Deibe, *RSC Adv.*, 2016, **6**, 103088–103094.
47 M. J. Schultz, R. S. Adler, W. Zierkiewicz, T. Privalov and M. S. Sigman, *J. Am. Chem. Soc.*, 2005, **127**, 8499–8507.
48 M. J. Schultz, C. C. Park and M. S. Sigman, *Chem. Commun.*, 2002, 3034–3035.
49 J. F. Hartwig, *Organotransitionmetal chemistry: from bonding to catalysis*, University Science Books, Sausalito, 2010.
50 L. Yang, D. R. Powell and R. P. Houser, *Dalton Trans.*, 2007, 955–964.
51 L. Ding, Z. Chu, L. Chen, X. Lü, B. Yan, J. Song, D. Fan and F. Bao, *Inorg. Chem. Commun.*, 2011, **14**, 573–577.
52 N. T. S. Phan, M. Van Der Sluys and C. W. Jones, *Adv. Synth. Catal.*, 2006, **348**, 609–679.
53 K. Yu, W. Sommer, J. M. Richardson, M. Weck and C. W. Jones, *Adv. Synth. Catal.*, 2005, **347**, 161–171.
54 M. L. Kantam, P. Srinivas, J. Yadav, P. R. Likhar and S. Bhargava, *J. Org. Chem.*, 2009, **74**, 4882–4885.
55 C. M. Frech, L. J. W. Shimon and D. Milstein, *Angew. Chem., Int. Ed.*, 2005, **44**, 1709–1711.
56 Q. Yao, M. Zabawa, J. Woo and C. Zheng, *J. Am. Chem. Soc.*, 2007, **129**, 3088–3089.
57 T. Wang, X.-Q. Hao, J.-J. Huang, K. Wang, J.-F. Gong and M.-P. Song, *Organometallics*, 2014, **33**, 194–205.
58 W. A. Carole and T. J. Colacot, *Chem. – Eur. J.*, 2016, **22**, 7686–7695.
59 G. Sheldrick, *Acta Crystallogr., Sect. A: Found. Adv.*, 2015, 3–8.
60 O. V. Dolomanov, L. J. Bourhis, R. J. Gildea, J. A. K. Howard and H. Puschmann, *J. Appl. Crystallogr.*, 2009, **42**, 339–341.
61 G. Sheldrick, *Acta Crystallogr., Sect. C: Struct. Chem.*, 2015, **71**, 3–8.
62 C. F. Macrae, I. Sovago, S. J. Cottrell, P. T. A. Galek, P. McCabe, E. Pidcock, M. Platings, G. P. Shields, J. S. Stevens, M. Towler and P. A. Wood, *J. Appl. Crystallogr.*, 2020, **53**, 226–235.